Reactive and Functional Polymers 181 (2022) 105444

Contents lists available at ScienceDirect

Reactive and Functional Polymers

journal homepage: www.elsevier.com/locate/react

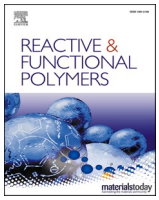

Are ultrafine submicron sized gliadin fibrous materials suitable as bio-absorbents? Processing and post-treatment derived structures and functional properties

Faraz Muneer [a,*], Mikael S. Hedenqvist [b], Ramune Kuktaite [a]

[a] Department of Plant Breeding, Swedish University of Agricultural Sciences, Box 190, SE-23422 Lomma, Sweden
[b] Department of Fibre and Polymer Technology, KTH Royal Institute of Technology, SE-100 44 Stockholm, Sweden

ARTICLE INFO

Keywords:
Electrospinning
Gliadin fibers
Protein crosslinking
Protein structure
Absorbents
Blood absorption

ABSTRACT

Gliadins were electrospun into ultrafine fibrous membrane-like materials to evaluate their processability and suitability as bio-absorbents. From a wide range of tested protein concentrations and processing conditions, 15 and 20% protein solutions were optimal to produce uniform fibers with sizes <1 μm. The results showed that the 20% gliadin solution produced uniform round fibers, while 15% gliadin solution resulted in formation of diverse morphologies such as round and flat-ribbon shaped fibers. Importantly, post-heat treatment of fibrous materials at 130 °C for 2 h increased crosslinking of gliadin protein and improved functionality of fibers. Heat-treatment induced formation of higher amounts of α-helices and random coils, though no change in β-sheets were observed. With post heat-treatment, the fibrous gliadin materials indicated crosslinking of proteins by inter and intra-molecular disulphide, hydrogen bonding and other weaker protein interactions. The newly fabricated gliadin fibrous material demonstrated certain stability and ability to absorb and "lock" defibrinated sheep blood, suggesting a support from submicron sized structural morphology of the material. For further development steps of gliadin-based fibrous materials, new efforts are needed in modification of gliadins to maintain the ultrafine structures and improve their strength in order to explore them as bio-absorbents or even scaffolds.

1. Introduction

In recent years, electrospinning has gained a huge interest as a cost effective and versatile method to produce fibrous materials from natural polymers for various applications [1]. For food (e.g. encapsulation of bioactive compounds), medical (wound dressings and control-release of drugs) and personal hygiene applications, proteins have been shown as a stand-out raw material for production of fibers and absorbent materials mainly due to their superior biodegradability, biocompatibility and functionality [1–3]. Among plant proteins, wheat gluten is a highly diverse polymer with inherent complex molecular structure which consists of low molecular weight monomeric gliadins, and low- and high-molecular weight polymeric glutenins [4]. The ratio between the gliadins and glutenins in wheat gluten provides it with unique visco-elasticity and intrinsic functionalities such as, ability to form fibers [5]. Wheat gluten's tunable structural and functional properties have been explored in a number of material applications e.g. films [6], foams [7], composites [8], superabsorbent particles [9] and electrospun microfibers [5,10].

Among different factors that influence electrospinability of a polymer solution and electrospun fibers morphology, are polymer concentration, molecular weight profile and suitable solvent [11]. For example, limited solubility of wheat gluten in polar or even reducing solvents largely due to the presence of high molecular weight glutenins fraction, complicates the electrospinning process [5]. In previous studies, wheat gluten was partially dissolved in different reducing solvents (urea) [2,12] and non-reducing solvent e.g. sodium dodecyl sulphate and sodium dihydrogen-phosphate combined with sonication to successfully produce electrospun fibers in the range of micro- and nano-scales [5]. Although, large part of glutenin polymeric fraction remain undissolved due to its molecular complexity e.g. high molecular weight and highly crosslinked protein network, which affected the overall protein spinability [5].

The significant advantage in using the major gliadin fraction with its lower molecular weight of proteins (28–55 kDa) compared to glutenins is that this fraction can be easily solubilized in 70% ethanol solution

* Corresponding author.
E-mail address: faraz.muneer@slu.se (F. Muneer).

https://doi.org/10.1016/j.reactfunctpolym.2022.105444
Received 2 August 2022; Received in revised form 11 October 2022; Accepted 22 October 2022
Available online 27 October 2022

making them an ideal candidate for fibrous materials [3,13]. Despite the previous studies, where gliadin-based electrospun fibers were produced for encapsulation of bioactive compounds for food applications [3,14,15], drug control release material [1] and amyloid-like fibrils [16,17], still a large knowledge gap exist of their unexplored potential in bio-based absorbent applications.

Unlike glutenins, the gliadins in their native form contain relatively lower amount of sulphur-rich amino acids and form exclusively intramolecular disulphide crosslinks [18]. When proteins are in solution, unfolding and disruption of weaker bonds takes place, and during electrospinning rapid evaporation of solvent results in reformation of inter- and intramolecular crosslinks among polypeptide chains to form fibers [19]. Since, electrospinning does not include heating or chemically aided crosslinking step to induce high degree of protein crosslinking among protein polypeptide chains, there is a strong tendency that produced gluten fibers seem to have insufficient mechanical performance, despite their attractive absorption properties of bio-liquids [5]. Regarding gliadins, another interesting aspect is their potential as scaffolding biomaterials [20], suggesting their attractiveness in absorbent applications. Although, a careful consideration of gliadin caused inflammatory reactions among susceptible individuals and gliadin materials relation to gluten-related disorders e.g. celiac disease should be carefully evaluated [21,22]. However, a more hands-on approach is needed in order to evaluate the gliadin based fibrous materials' potential in absorbent applications. This requires new knowledge on fibrous gliadin materials' functionalities, as well as regarding improvement of functional properties of these materials.

In this study, electrospinning experiment was first conducted to determine the electrospinnable window of gliadin fibrous materials using different conditions in order to develop new materials with diverse absorption properties. The main objective of this study was to determine the structural properties of proteins and morphology of newly developed gliadin fibrous materials and assess their absorption properties. In addition, we also studied the impact of post-heat treatment on gliadin crosslinking, secondary structure, and functional performance of the fibrous materials.

2. Materials and methods

2.1. Materials

Industrial wheat gluten (WG) powder was purchased from Lantmännen Reppe AB, Lidköping, Sweden, with reported protein content of 77.7%, starch 5.8%, moisture 6.9% and fat content of 1.2%, according to the supplier, which was further used for gliadin production.

2.2. Methods

2.2.1. Separation of gliadins from wheat gluten

Gliadin fraction was separated from WG using a method described by Muneer et al., [23] and Kuktaite et al., [24]. Briefly, 16 g of WG powder was dispersed in 200 ml of ethanol (70%) using a metal sieve to avoid clump formation. The dispersion was constantly stirred until the mixture was homogenous. Thereafter, dispersion was placed on a shaker (IKA-KS 500, IKA, Germany) for 30 min at 300 rpm and later centrifuged for 10 min at 10000 rpm in Sorvall RC 6+ centrifuge (Thermo Scientific, U.S.A) to collect the ethanol soluble gliadin fraction. A rotary evaporator (Buchi, Switzerland) equipped with a vacuum pump was used to collect the gliadin fraction at 45 ± 2 °C. The collected gliadin fraction was lyophilized and ground to powder using an IKA A-10 yellow mill (IKA, Germany). The protein content of gliadin was 91%, determined according to Dumas method [25].

2.2.2. Sample preparation and electrospinning

Two electrospinning solutions of gliadin with diverse concentrations were prepared by dissolving 15 and 20% protein (*w*/w %) in 70% ethanol. Gliadin powder was slowly added to ethanol using a metal sieve to avoid clump formation and stirred for at least 2 h to completely dissolve the proteins. An electrospinning apparatus equipped with a high voltage supply (Spellman SL60, USA) and precision controlled pump (SAGE Orion M362, Thermo Scientific, U.S.A) was used to electrospun gliadin solution. Protein solution was filled in a 10 ml syringe, the positive terminal of the high voltage supply was connected to a metal blunt needle (1 mm gauge opening), and negative terminal was connected to a collection target (aluminum foil). A high voltage of 15 kV was used to pull electrospinning solution to the target at a predetermined distance of 10 cm and at a constant flow rate of 0.5 ml/h. The electrospun gliadin fibers were removed from the aluminum foil and stored in an airtight box until further analysis. To determine the moisture content of gliadin fibers, 50 mg of material was placed in an oven at 105 °C for 24 h and weight difference yielded the moisture content (Table 1).

2.2.3. Scanning electron microscopy

To study the morphology of electrospun gliadin fibers, samples of ca. 1 cm^2 were mounted on a metal stub and sputter coated with gold for 40 s in a Cressington 108 auto, using a 20 mA voltage. Coated samples were studied in a scanning electron microscope (Hitachi, SU3500, Japan) using an acceleration voltage of 5 kV.

2.2.4. Heat-treatment of electrospun fibers

To induce and promote protein polymerization and crosslinking among protein polypeptide chains, the gliadin fibers were heat-treated at 130 °C in an oven for 2 h. Samples were removed from the oven and stored in an airtight container at room temperature until further analysis.

2.2.5. Protein solubility analysis by SE-HPLC

Size exclusion-high performance liquid chromatography (SE-HPLC) was performed to evaluate protein solubility and size distribution (polymerization) using a method described by Muneer et al., [5] with some modifications. A Waters 2690 Separation Module (Waters, USA) equipped with a Biosep-SEC-S 4000 (Phenomenex, USA) column was used to separate proteins. A sample of 5 ± 0.05 mg was added to 1.4 ml SDS-phosphate extraction buffer (0.5% SDS, 0.05 M NaH_2PO_4, pH 6.9) in 1.5 ml Eppendorf tubes. Tubes with samples were vortexed for 10 s in a Whirli Vib 2 (Labassco, Sweden) at full speed and thereafter, agitated for 5 min in a IKA Vibrax VXR (IKA, Germany) at 2000 rpm. All the samples were centrifuged at 12500 rpm for 30 min and supernatant was collected as first extraction (1Ex). In the second extraction, the 1.4 ml buffer was added to the pellet from 1Ex and sonicated for 30 s in a Sanyo Soniprep 150 (Tamro, UK) followed by centrifugation at 12500 rpm for 30 min. The supernatant was collected in HPLC vials and designated as 2Ex. Third extraction (3Ex) was only performed for heat-treated samples when a relatively very small pellet was observed after the 2Ex. For 3Ex, 1.4 ml buffer was added to the pellet from 2Ex followed by two sonication intervals of 30 and 60 s. Thereafter, samples were centrifuged and supernatant was collected in HPLC vials and designated as 3Ex. For analysis of each sample, 20 µl was injected at an isocratic flow of 0.2 ml/min (50% acetonitrile, 0.1% TFA; 50% H_2O, 0.1% TFA) for 30 min. Chromatograms were obtained by UV-detection at a wavelength of 210 nm using a Waters 996 Photodiode Array Detector (Waters, USA).

Table 1
Moisture content in electrospun gliadin and wheat gluten (WG)* fibers (Muneer et al. 2022).

	Moisture content %
WGF15	8.41 (0.39)*
WGF20	6.85 (0.04)*
Gli15	3.51 (0.23)
Gli20	3.93 (0.41)

Chromatograms were integrated and divided into two groups, polymeric proteins (PP, retention time 7–14 min) and monomeric proteins (MP, 14–28 min).

2.2.6. Fourier transform infrared (FT-IR) spectroscopy

FT-IR spectroscopy analysis was carried using a Spectrum 2000 FT-IR spectrometer (Perkin-Elmer Inc., USA) equipped with a single reflection ATR (Golden Gate, Speac Ltd.). All the samples were dried for at least 72 h in a desiccator prior to analysis. Data was obtained from 32 consecutive scans between 4000 and 600 cm^{-1} with a scanning resolution of 4.0 cm^{-1}. Spectrum software was used to Fourier self-de-convolute the obtained data using a smoothing factor of 2 and 70%, and an enhancement factor (γ). A Savitzky–Golay 5-point second-order derivative analysis was performed on all the samples to find underlying corresponding peaks to determine secondary structure [23]. Spectra from each sample was base-line corrected and peak fitting was performed using Fityk software (version 1.3.1).

2.2.7. Blood absorption

To analyze the blood absorption behavior, round disks of 10 mm in circumference were cut from gliadin electrospun fiber films. Each disk weighed in duplicates prior to the test. To visually monitor the blood absorption, defibrinated sheep blood two times the weight of the sample was dropped on the surface of the disks with help of a pipette. Thereafter, samples were left to dry at room temperature for 1 h. Pictures were taken to record the blood flow and absorption by the fiber disks.

3. Results and discussion

3.1. Morphology of gliadin fibrous materials

Wheat gluten (WG) proteins among other natural polymers provide a narrow window for preparation of electrospinnable working fluids to produce good quality electrospun fibers, although gliadins are more processing "friendly" to make fibers [26]. The most important factors for successful electrospinning include appropriate polymer concentration and suitable solvent. In this study, ethanol (70%) was used as a solvent in a series of different gliadin concentrations (5, 10, 15, 20 and 25% *w/v*), in which 15 and 20% gliadin were the most suitable for electrospinning in order to produce good flexible fibrous films (Fig. 1). These fibrous films were white in color and resembled a membrane, and overall were very different in appearance when compared to the three dimensional WG cotton-like electrospun fibers produced in Muneer et al. [5]. The initial moisture content of gliadin fibers was lower than of the previously WG-cotton like fibrous materials (Table 1). The lower moisture content in gliadin fibers could be a result of smaller sized fibers compared to WG fibers, which offer smaller surface area for water absorption. In this study, no fibers were produced at lower gliadin concentrations (5 and 10%), probably due to lower amounts of physical chain entanglements between the polypeptide chains that form fibers, similar to what has been observed in the previous studies [1,14,15]. At higher gliadin concentration (e.g. 25%), the spinning solution became too viscose and protein fell out of solution during the spinning process, making the spinning operation very complex. It is also known that the electrical conductivity of the solution of 25% or higher concentration of gliadins (up to 35 wt%) reduces due to limited electron mobility and the high viscosity of solution [15]. Electrospun fiber films obtained with 15 and 20% gliadins were relatively flexible membrane-like materials, as they showed ability to be rolled or bent without being damaged (Fig. 1b), and were later used for further analysis.

Scanning electron micrographs of both GliF15 and GliF20 fibrous films showed randomly arranged fibrous networks and varying fiber morphologies (Fig. 2). Spinning dope with both protein concentrations used (e.g. 15 and 20%), yielded electrospun fibers with rather similar fiber diameter ($\leq$ 1 μm) and morphology (Fig. 2). The GliF15 fibers showed a mix of round and flat ribbon-like fiber morphologies (Fig. 2b, solid red arrows show flat fiber morphology), as compared to GliF20 with round fibers (Fig. 2d, white arrows). In GliF15 fibrous material, a flat ribbon-like morphology was a result of rapid evaporation of solvent while reaching the target, and also due to the lower amount of proteins in the spinning dope, suggesting the lower probability of protein entanglements to maintain the round fiber morphology as shown in the previous studies [10,12]. The production of flat ribbon-like fibers significantly increased when the 15% gliadin spinning dope was spun at a needle to target distance of 15 cm vs 10 cm (Fig. 2e-f compared to a-d). This suggests that needle to target distance also plays an important role in determining fiber morphology, especially at lower gliadin concentrations e.g. 15%. An impact of lower protein concentration (e.g. 15 vs. 20%) on fiber morphology has been previously reported in WG and gliadin based electrospun fibers [1,5,12].

In general, spinning dope with higher protein concentration produced higher amount of electrospun fibers than the lower protein concentration samples during the same time. In this study, this was evident with electrospun fibers of 20% gliadin covering target surface relatively faster versus 15% gliadin fibers within similar spinning times. This suggests, that higher protein concentration contributes with higher amount of unfolded proteins chains hence increasing the probability of higher amount of physical chain entanglements and leading to smooth spinning operation with round fibers [10].

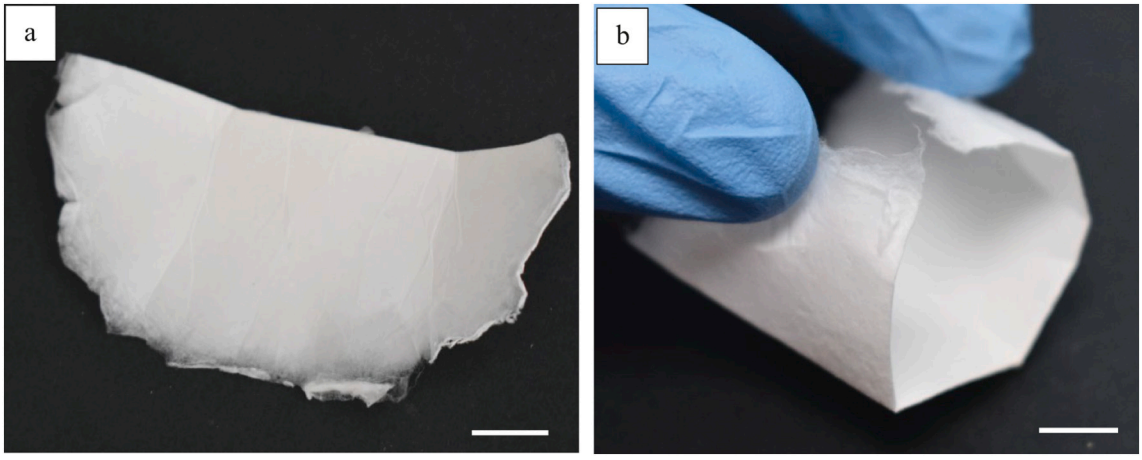

Fig. 1. Representative images of electrospun fibrous films made from 20% gliadin protein concentration; a piece of gliadin electrospun fibrous film (a) and rolled fibrous film indicating flexibility and membrane-like thickness (b), bar is 1 cm.

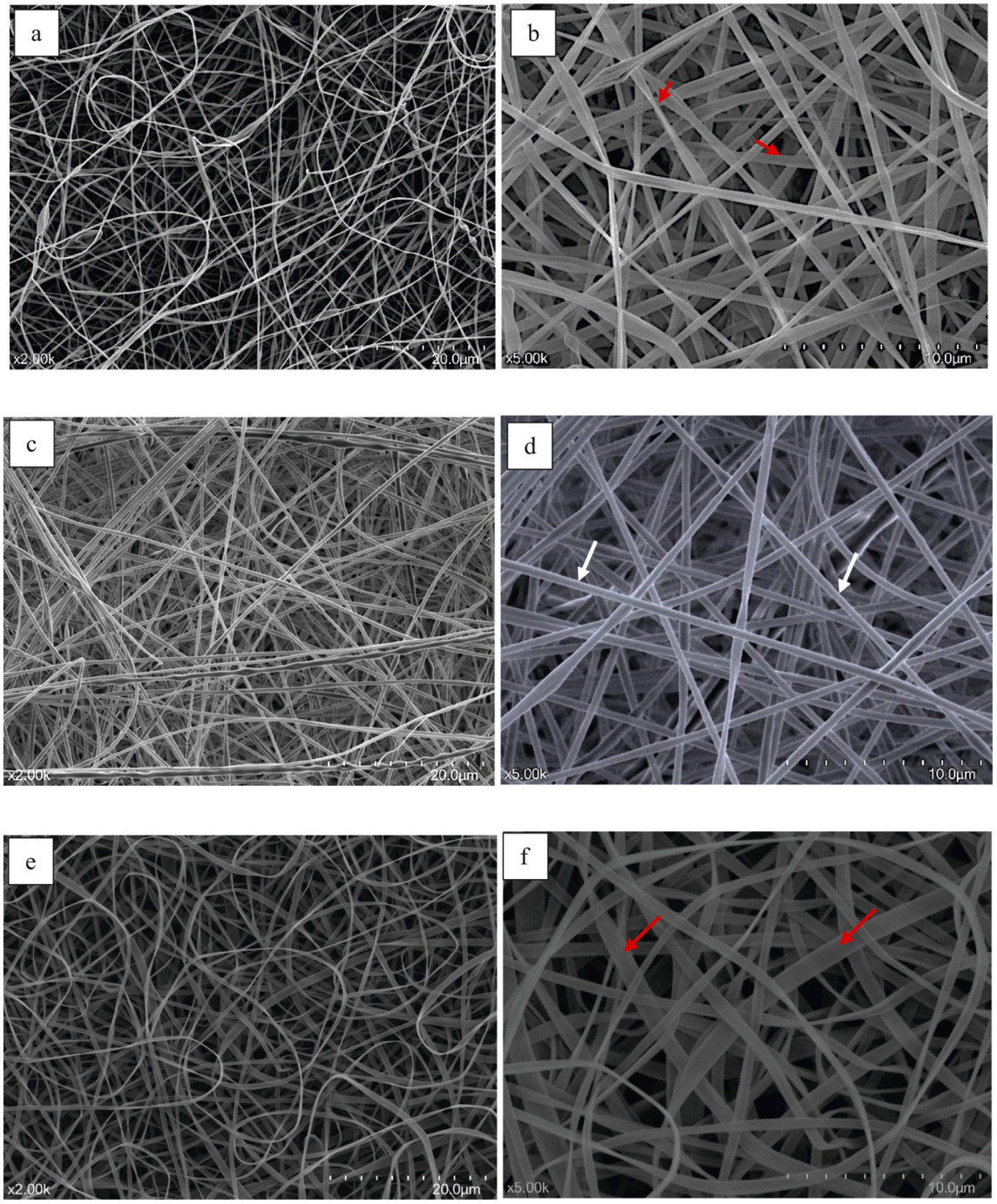

Fig. 2. Scanning electron micrographs of electrospun gliadin fibrous materials produced from two different protein concentrations, GliF15 (a, b), GliF20 (c, d), spun at 10 cm needle to target distance, and (e, f) GliF15 fibers, spun at needle to target distance of 15 cm.

3.2. Protein polymerization of spinning solutions and different fibrous materials

3.2.1. Gli15 and Gli20 fibrous materials

The protein solubility analysis on the protein films was performed to evaluate protein polymerization during fiber formation and after heat-treatment of fibers at 130 °C. A representative SE-HPLC chromatogram showed a decrease in overall protein solubility in non-heat treated and heat-treated fibers compared to gliadin powder and protein spinning solutions after the 1Ex(Fig. 3a). The SE-HPLC data analysis showed that during 1Ex, the largest amounts of both polymeric (PP) and monomeric proteins (MP) were extracted in Sol-Gli15 and Sol-Gli20 as compared to gliadin powder (Fig. 3b). The largest amounts of both PP and MP fractions in gliadin solutions was a result of unfolding and rearrangement of protein polypeptide chains in solution state. Whereas, during electrospinning these unfolded protein chains re-crosslinked to form fibers as shown by the decreased protein solubility of both PP and MP fractions in fiber samples (Fig. 3c). In their native form, the wheat proteins exist as coiled or folded chains maintained by disulphide crosslinks between cysteine residues and other weaker protein interactions e.g. hydrogen bonding and ionic interactions [27]. Gliadins, due to their lower molecular weight than glutenins are known to completely dissolve in ethanol (70%), which means that disruption and stretching of weaker protein interactions occur in solution state.

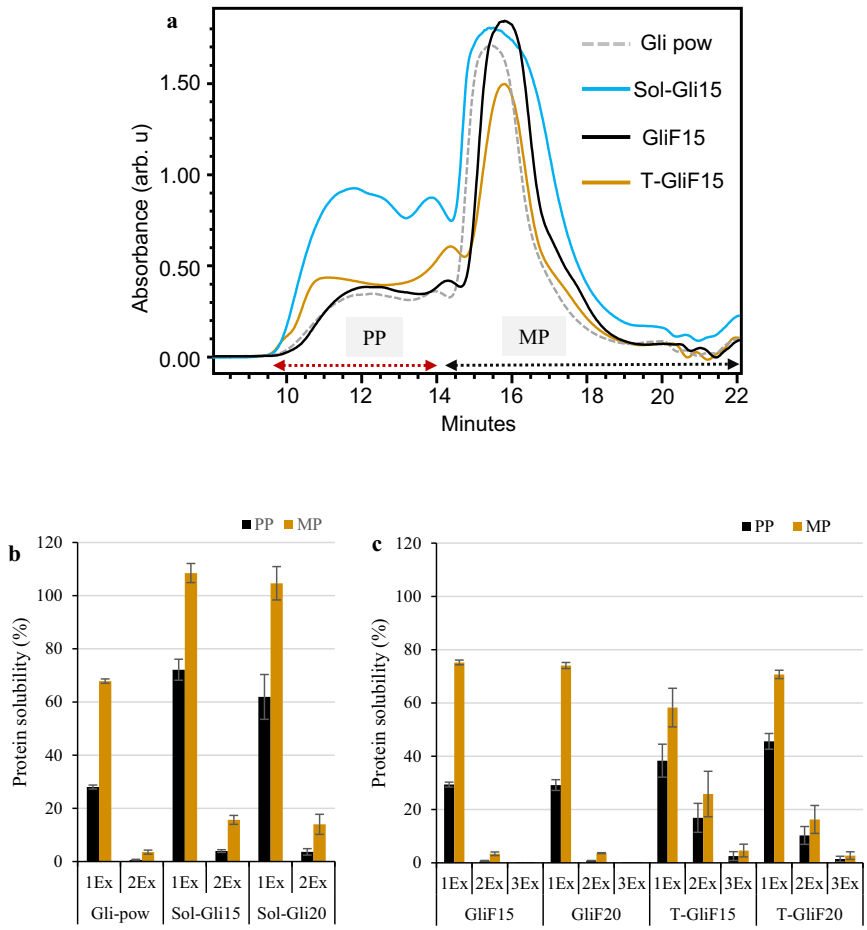

Fig. 3. Representative chromatograms of first extraction (1Ex) of gliadin powder (a) (Gli-pow), spinning solution (Sol-Gli15), electrospun fibers (GliF15) and heat-treated fibers (T-GliF15) showing protein solubility profile, and (b) protein solubility of Gli-pow, Sol-GliF15 and Sol-Gli20, and (c) non-treated (GliF15 and GliF20) versus heat-treated (T-GliF15 and T-GliF20) fibrous films. PP; polymeric protein and MP; monomeric proteins.

However, when rapid evaporation of the solvent occurs during electrospinning, proteins reform inter and intramolecular disulphide crosslinks via thiol/disulphide interchange reactions and form fibers [15,19]. In case of 15 vs 20% of gliadin fibrous film solubility, slightly lower though insignificant protein extractability was observed in GliF20 (Fig. 3b) indicating greater protein aggregation, where hydrogen interactions between C═O and N—H bonds of gliadin could took place, as similarly observed in the gliadin fiber films with cuminaldehyde [28].

3.2.2. *Temperature induced crosslinking of Gli15 and Gli20 fibrous materials*

The non-heat treated GliF15 and GliF20 fibrous materials showed similar protein solubility, as indicated by similar amounts of extracted PP and MP during 1Ex and 2Ex (Fig. 3c). In heat-treated fibers (T-GliF15 and T-Gli20), relatively higher amount of PP fraction was extracted during the 1Ex compared to non-treated fibers, which suggest that post-heat treatment increased protein interaction among polypeptide chains. Similarly, a relative decrease in MP fraction during 1Ex in heat-treated versus non-treated fibers indicated that MP fraction became part of larger protein network upon heating (Fig. 3c). A relative decrease in MP fraction during 1Ex suggests that smaller proteins fraction became part of larger protein network upon heat-treatment. After the 2Ex, higher amount of both PP and MP fraction was extracted in heat-treated fibers compared to non-treated samples, which suggest that the heat-treatment contributed to increased proteins interactions maintained by disulphide crosslinks, which were only broken down with sonication treatment. Previous studies have shown that heat-treatment of gluten protein contribute to increased protein aggregation and crosslinking upon heating, where smaller protein becomes part of larger protein network and even irreversible bonds are formed which make proteins insoluble [5,29,30]. However, in this study, the extent of protein crosslinking and aggregation was lower as compared to compression molded or extruded wheat gluten materials produced in previous studies.

In non-treated fibers (i.e. GliF15 and Gli20), the PP and MP fractions were extracted during the first extraction, which shows that fiber formation was a result of proteins crosslinking largely maintained by hydrogen bonding and other weaker protein interactions between polypeptide chains which were easily broken with SDS treatment during 1Ex. Whereas in heat-treated fibers some of PP and MP fractions were extracted during 2Ex and 3Ex, which suggest that heat-treatment induced a higher degree of protein crosslinking maintained by both intra- and intermolecular disulphide crosslinks (Fig. 3b) and hydrogen bonding. A similar phenomenon was observed among WG based electrospun fibers, which suggests that heat-treatment was necessary to induce higher degree of protein crosslinking among proteins [5].

3.3. *Protein secondary structure of electrospun fibers by FT-IR*

Changes in molecular conformation of gliadin protein after electrospinning in GliF15, GliF20, T-GliF15, T-GliF20 and gliadin powder were analyzed using FT-IR spectroscopy. The protein secondary structure of relevant peaks arising from the amide bonds stretching vibrations (of C═O and N—H bonds) was studied in amide I region (1600–1700 cm^{-1}) for all the samples are presented in Fig. 4. For the studied samples, relative sizes of peaks indicating secondary structures such as, α-helices, random coils and β-sheets conformations were determined by

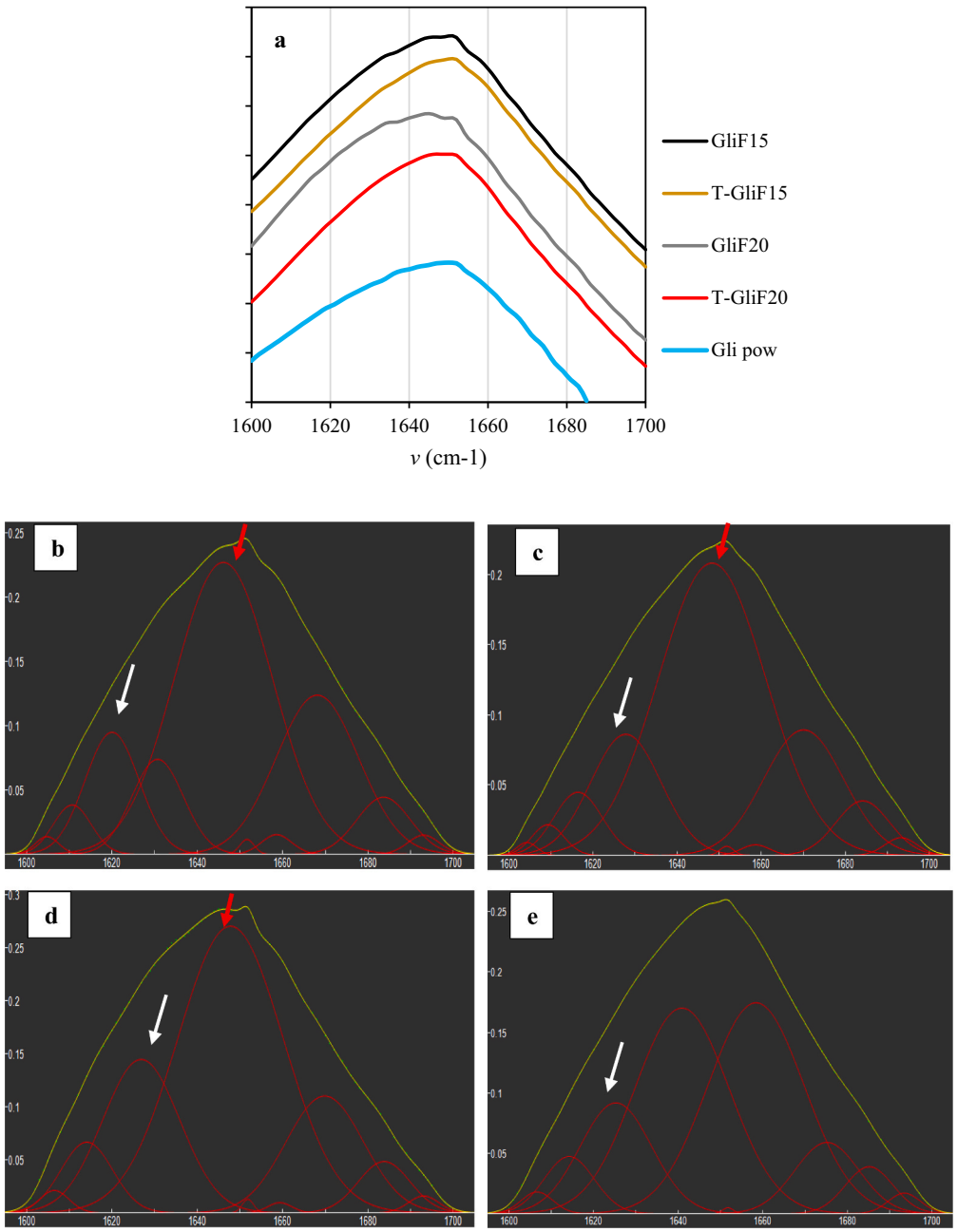

Fig. 4. Protein secondary structure profile of gliadin powder (Gli pow), non-treated (Gli15 and GliF20) and heat-treated (T-Gli15 and T-GliF20) gliadin electrospun fibers and Gaussian curve fitting of individual FT-IR profile of b) GliF15, c) T-GliF15, d) GliF20 and e) T-GliF20.

comparing the relative size/intensity of peak shoulders in the regions 1645–1660 and 1600–1625 cm^{-1}, respectively [30]. When comparing the spectra of unprocessed gliadin powder with those of fibrous materials, a relatively higher-intensity peak in the region 1645–1660 cm^{-1} indicating the presence of α-helices/random coils was present among all the fiber samples (Fig. 4a). However, for all the studied gliadin samples, the peak intensity between 1600 and 1625 cm^{-1} was rather same (Fig. 4a).

To further investigate the nature of secondary structures, peak fitting was performed for each spectrum to study the underlying structural peaks which were unclear due to very small differences among all the samples (Table 2 and Fig. 4b-e). Peak fitting analysis confirmed that the β-sheets conformational peaks between (1615–1630 cm^{-1}) did not largely shift among all the heat-treated and non-treated fibers (Fig. 4b-e, white arrows). A high intensity peak in region 1645–1660 cm^{-1} showed the presence of α-helices/random structures among all the samples (Fig. 4b-e, red arrows). In T-GliF20 sample, two peaks were observed in 1640–1660 cm^{-1} region showing the presence of both unordered structures and α-helices (Fig. 4e). The formation of α-helices/random structures in normal and heat-treated fibers have previously been observed in WG electrospun fibers [5,31]. Important to note, from a recent study of gelatin-gliadin nano-fibers probed by circular dichroism (CD), a major negative band in the 200–210 nm range associated with α-helix and an increase in β-sheet structure with increase in gliadin concentration in the blend were observed by Chen et al. [32].

These results indicated that fiber formation during electrospinning and post-heat crosslinking of fibers only contributed to the formation of α-helices/random structures maintained by hydrogen bonding and disulphide crosslinks (especially in heat-treated fibers) between the protein polypeptide chains as also observed in SE-HPLC results (Fig. 3b).

Table 2
FT-IR de-convoluted absorbance spectra and relative amounts (%) of different secondary structures present in gliadin fiber samples.

Peak	Assignment	GliF15	T-GliF15	GliF20	T-GliF20
1605 (1.1)	β-sheets	0.6	0.4	1.1	1.1
1609 (1.0)	β-sheets	3.1	1.7	0	0
1616 (2.7)	β-sheets	11.1	5.2	6.1	4.8
1626 (1.2)	β-sheets; strongly hydrogen bonded peptide groups	0	14.6	19.9	13.4
1630	β-sheets; weakly hydrogen bonded peptide groups	8.2	0	0	0
1643 (3.7)	Unordered	0	0	0	33.1
1648 (0.3)	α-helices and random coils	47.5	53.9	51.2	0
1658 (0.4)	α-helices	1.0	0.5	0.4	34.5
1670 (3.1)	β-turns	21.9	17.3	15.3	7.7
1684 (0.7)	β-sheets; weakly hydrogen bonded peptide groups	5.1	5.1	4.5	3.7
1693 (0.2)	β-turns	1.1	0.9	0.8	1.1

A similar change in structural conformation specifically related to formation of α-helices and random coils during electrospinning of protein into fibers has been reported in gliadins and other proteins [15,33]. Whereas, a relatively low to no change in 1600–1625 cm^{-1} in peak intensity showing β-sheets, indicated the preservation of β-sheets' conformation during electrospinning and fiber heat-treatment, which has previously been reported in WG based electrospun fibers [2,5,15].

3.4. Blood absorption of fibrous materials

To analyze the blood absorption of gliadin fibrous materials, samples were cut into 1 cm^2 disks and the defibrinated sheep blood two times the weight of the fibrous disk was poured on the surface of the disks (Fig. 5). The visual observation showed that the blood was absorbed by the fibrous disk, however the physical structure of the disk collapsed after blood absorption and it was difficult to retrieve it for weight measurements (Fig. 5). A representative image of T-GliF20 fibrous disk showed the typical blood absorption behavior (Fig. 5). When blood drops were placed on the surface of fibrous disk, they stayed on the surface for a few seconds before spreading through the fibrous network (Fig. 5a).

After 30 min, fibrous disk shrunk and blood stayed within the boundaries of the sample and dried out. A similar blood absorption behavior was observed in electrospun WG fibrous films [5], despite different physical appearance (membrane-like materials vs. 3D cotton-like materials). The brief retention of the blood on the surface of the films can be explained by the intrinsic hydrophobic nature of gliadin and uneven surface of the fibrous film, as well as exposure of hydrophobic peptide residues to the surface of the fibers [2]. Whereas the retention of the blood within the boundaries of fibrous disc can be due to increased water stability of the fibers facilitated by an increased protein cross-linking (conversion of SH to S—S bonds) after heat-treatment, as shown in WG fibrous materials [2,5]. This blood absorption phenomenon of gliadin electrospun fibers could be further explored as medical membranes (Fig. 5c). It is important to note that gliadin material was able to stay intact when submerged in water for 24 h (results not shown). However, there is need to further improve the functional properties e.g. strength, flexibility and liquid absorption capacity for successful medical absorbent or scaffold applications [34]. In addition, to further increase our understanding on liquid absorption behavior of protein-based electrospun fibers with various fiber morphologies (i.e. flat-ribbon like fibers vs. round fibers) would be of interest to explore in further studies.

During last decade, efforts have been made to improve superabsorbent capacity of WG proteins by various protein crosslinking aids (e.g. heating and chemical additives) and functionalization (e.g. chemically modifying protein functional groups) for medical and personal hygiene applications [35–37]. The results have shown that the functionalized WG particles can absorb up to 4000% of water and 250% of sheep blood, which makes it a green alternative to petroleum-based superabsorbent materials used in personal hygiene applications [35]. Therefore, to improve water absorption capacity and stability of fibrous materials produced from WG proteins, a similar route can be adopted, where proteins are functionalized before fiber making process. These fibrous materials produced from biopolymers are required to have specific functional properties e.g. high surface area, porosity, and absorption capacity when used as absorbents for fluids in various health care and personal hygiene products [38,39].

4. Conclusions

In this study, different gliadin concentrations in aqueous ethanol (70%) were tested to establish a spinnable window to produce uniform sized and randomly arranged fibrous materials. Two gliadin protein concentrations 15 and 20%, produced uniform sized (≤1 μm) electrospun fibers. The fibrous films were white, porous (1–3 μm) and resembled a flexible membrane-like material. The protein concentration lower than 10% did not produce any fibers and protein concentration higher than 20% resulted in higher viscosity and protein falling out of solution, which made the electrospinning process complicated. Production of electrospun fibers was relatively smooth and fast from 20% protein concentration compared to 15%. Fibers produced from gliadin 20% concentration had round fiber morphology compared to a mix of round and flat-ribbon like morphology in lower protein concentration (15%) samples. This suggests that the protein concentration played a significant role in smooth electrospinning operation and enough protein chain entanglements to produce uniform fiber morphology.

Post-heat treatment (130 °C for 2 h) of electrospun fibers induced a higher degree of protein crosslinking in heat-treated samples compared to non-treated ones. Heat-treatment of electrospun fibers also contributed to relatively higher amount of α-helices and random coil structure in proteins, although β-sheets conformation showed low to relatively no change among both heat-treated and non-treated fibrous samples. This suggests that heat-treatment did contribute to increased protein cross-linking although not to an extent that would promote higher amount of β-sheets structure. Gliadin fibrous materials also showed that porous structure absorb the blood and fiber structure keeps it within its boundaries. However, there is need to further improve the functional properties (e.g. strength, flexibility and liquid absorption capacity, as well as ability to withstand long submersion in different bio-liquids) of fibrous materials either by protein functionalization and adding functional groups to the polypeptide chains, and by post-chemical cross-linking to make them suitable for medical and personal hygiene applications.

Data availability

The data used to support the finding of this study will be available on request from the corresponding author.

CRediT authorship contribution statement

Faraz Muneer: Data curation, Formal analysis, Methodology, Software, Validation, Visualization, Writing – original draft. **Mikael S. Hedenqvist:** Writing – review & editing. **Ramune Kuktaite:** Conceptualization, Funding acquisition, Project administration, Writing – review & editing.

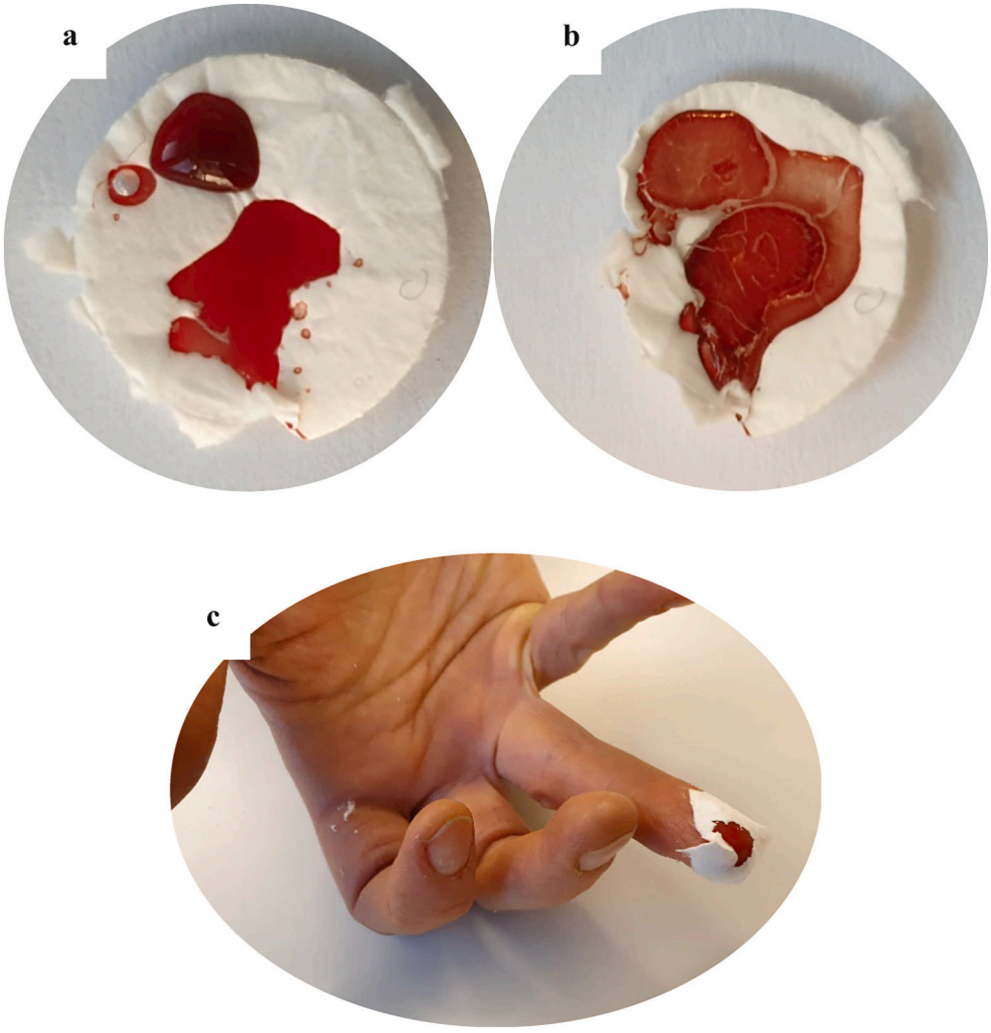

Fig. 5. The GliF20 fibrous material with defibrinated sheep blood; (a) two times of the actual weight of the fibrous film with freshly applied blood, (b) fibrous film shrinking after 30 min of contact with blood, (c) fibrous film used for blood absorption from the freshly wounded finger (R. Kuktaite's bleeding finger wrapped with gliadin film).

Declaration of Competing Interest

Authors declare no competing interests.

Data availability

Data will be made available on request.

Acknowledgements

This study was funded by the Swedish Research Council (FORMAS 2015-1052) and Swedish Governmental Research program Trees and Crops for Future. Mikael Sundin (RISE, Stockholm) is acknowledged for technical assistance with electrospinning equipment. Xinchen Ye is acknowledged for help and assistance for FT-IR analysis at Department of Fiber and Polymer Technology, KTH Royal Institute of Technology, Stockholm, Sweden.

References

[1] Y. Xu, J.-J. Li, D.-G. Yu, G.R. Williams, J.-H. Yang, X. Wang, Influence of the drug distribution in electrospun gliadin fibers on drug-release behavior, Eur. J. Pharm. Sci. 106 (2017) 422–430.

[2] H. Xu, S. Cai, A. Sellers, Y. Yang, Electrospun ultrafine fibrous wheat glutenin scaffolds with three-dimensionally random organization and water stability for soft tissue engineering, J. Biotechnol. 184 (2014) 179–186.

[3] N. Sharif, M.-T. Golmakani, M. Niakousari, S.M.H. Hosseini, B. Ghorani, A. Lopez-Rubio, Active food packaging coatings based on hybrid electrospun gliadin nanofibers containing ferulic acid/hydroxypropyl-beta-cyclodextrin inclusion complexes, Nanomaterials 8 (11) (2018) 919.

[4] E. Johansson, A.H. Malik, A. Hussain, F. Rasheed, W.R. Newson, T. Plivelic, M. S. Hedenqvist, M. Gällstedt, R. Kuktaite, Wheat gluten polymer structures: the impact of genotype, environment, and processing on their functionality in various applications, Cereal Chem. J. 90 (4) (2013) 367–376.

[5] F. Muneer, M.S. Hedenqvist, S. Hall, R. Kuktaite, Innovative green way to design biobased electrospun fibers from wheat gluten and these fibers' potential as absorbents of biofluids, ACS Environ. Au 2 (3) (2022) 232–241.

[6] R. Kuktaite, T.S. Plivelic, H. Türe, M.S. Hedenqvist, M. Gällstedt, S. Marttila, E. Johansson, Changes in the hierarchical protein polymer structure: urea and temperature effects on wheat gluten films, RSC Adv. 2 (31) (2012) 11908–11914.

[7] T.O. Blomfeldt, R. Kuktaite, T.S. Plivelic, F. Rasheed, E. Johansson, M. S. Hedenqvist, Novel freeze-dried foams from glutenin-and gliadin-rich fractions, RSC Adv. 2 (16) (2012) 6617–6627.

[8] Q. Wu, J. Rabu, K. Goulin, C. Sainlaud, F. Chen, E. Johansson, R.T. Olsson, M. S. Hedenqvist, Flexible strength-improved and crack-resistant biocomposites based on plasticised wheat gluten reinforced with a flax-fibre-weave, Compos. A: Appl. Sci. Manuf. 94 (2017) 61–69.

[9] A.J. Capezza, F. Muneer, T. Prade, W.R. Newson, O. Das, M. Lundman, R.T. Olsson, M.S. Hedenqvist, E. Johansson, Acylation of agricultural protein biomass yields biodegradable superabsorbent plastics, Commun. Chem. 4 (1) (2021) 52.

[10] D.L. Woerdeman, S. Shenoy, D. Breger, Role of chain entanglements in the electrospinning of wheat protein-poly (vinyl alcohol) blends, J. Adhes. 83 (8) (2007) 785–798.

[11] R. Pérez-Masiá, A. López-Rubio, J.M. Lagarón, Development of zein-based heat-management structures for smart food packaging, Food Hydrocoll. 30 (1) (2013) 182–191.
[12] D.L. Woerdeman, P. Ye, S. Shenoy, R.S. Parnas, G.E. Wnek, O. Trofimova, Electrospun fibers from wheat protein: investigation of the interplay between molecular structure and the fluid dynamics of the electrospinning process, Biomacromolecules 6 (2) (2005) 707–712.
[13] N. Reddy, Y. Li, Y. Yang, Wet cross-linking gliadin fibers with citric acid and a quantitative relationship between cross-linking conditions and mechanical properties, J. Agric. Food Chem. 57 (1) (2009) 90–98.
[14] P.K. Akman, F. Bozkurt, M. Balubaid, M.T. Yilmaz, Fabrication of curcumin-loaded gliadin electrospun nanofibrous structures and bioactive properties, Fibers Polym. 20 (6) (2019) 1187–1199.
[15] N. Sharif, M.-T. Golmakani, M. Niakousari, B. Ghorani, A. Lopez-Rubio, Food-grade gliadin microstructures obtained by electrohydrodynamic processing, Food Res. Int. 116 (2019) 1366–1373.
[16] T.J. McMaster, M.J. Miles, D.D. Kasarda, P.R. Shewry, A.S. Tatham, Atomic force microscopy of A-gliadin fibrils and in situ degradation, J. Cereal Sci. 31 (3) (2000) 281–286.
[17] M. Monge-Morera, M.A. Lambrecht, L.J. Deleu, N.N. Louros, F. Rousseau, J. Schymkowitz, J.A. Delcour, Heating wheat gluten promotes the formation of amyloid-like fibrils, ACS Omega 6 (3) (2021) 1823–1833.
[18] H. Wieser, Chemistry of gluten proteins, Food Microbiol. 24 (2) (2007) 115–119.
[19] J. Dong, A.D. Asandei, R.S. Parnas, Aqueous electrospinning of wheat gluten fibers with thiolated additives, Polymer 51 (14) (2010) 3164–3172.
[20] S. Voci, M. Fresta, D. Cosco, Gliadins as versatile biomaterials for drug delivery applications, J. Control. Release 329 (2021) 385–400.
[21] K.M. Lammers, M.G. Herrera, V.I. Dodero, Translational chemistry meets gluten-related disorders, ChemistryOpen 7 (3) (2018) 217–232.
[22] G. Caio, U. Volta, A. Sapone, D.A. Leffler, R. De Giorgio, C. Catassi, A. Fasano, Celiac disease: a comprehensive current review, BMC Med. 17 (1) (2019) 142.
[23] F. Muneer, M. Andersson, K. Koch, M.S. Hedenqvist, M. Gällstedt, T.S. Plivelic, C. Menzel, L. Rhazi, R. Kuktaite, Innovative gliadin/glutenin and modified potato starch green composites: chemistry, structure, and functionality induced by processing, ACS Sustain. Chem. Eng. 4 (12) (2016) 6332–6343.
[24] R. Kuktaite, W.R. Newson, F. Rasheed, T.S. Plivelic, M.S. Hedenqvist, M. Gällstedt, E. Johansson, Monitoring nanostructure dynamics and polymerization in glycerol plasticized wheat gliadin and glutenin films: relation to mechanical properties, ACS Sustain. Chem. Eng. 4 (6) (2016) 2998–3007.
[25] S. Serrano, F. Rincón, J. García-Olmo, Cereal protein analysis via dumas method: standardization of a micro-method using the EuroVector elemental analyser, J. Cereal Sci. 58 (1) (2013) 31–36.
[26] N. Reddy, Y. Yang, Self-crosslinked gliadin fibers with high strength and water stability for potential medical applications, J. Mater. Sci. Mater. Med. 19 (5) (2008) 2055–2061.
[27] I. Rombouts, B. Lagrain, M. Brunnbauer, P. Koehler, K. Brijs, J.A. Delcour, Identification of isopeptide bonds in heat-treated wheat gluten peptides, J. Agric. Food Chem. 59 (4) (2011) 1236–1243.
[28] M.M. Hajjari, M.-T. Golmakani, N. Sharif, Fabrication and characterization of cuminaldehyde-loaded electrospun gliadin fiber mats, LWT 145 (2021), 111373.
[29] T.O.J. Blomfeldt, R. Kuktaite, E. Johansson, M.S. Hedenqvist, Mechanical properties and network structure of wheat gluten foams, Biomacromolecules 12 (5) (2011) 1707–1715.
[30] F. Muneer, M. Andersson, K. Koch, C. Menzel, M.S. Hedenqvist, M. Gällstedt, T. S. Plivelic, R. Kuktaite, Nanostructural morphology of plasticized wheat gluten and modified potato starch composites: relationship to mechanical and barrier properties, Biomacromolecules 16 (3) (2015) 695–705.
[31] C. Liu, X. Ma, Study on the mechanism of microwave modified wheat protein fiber to improve its mechanical properties, J. Cereal Sci. 70 (2016) 99–107.
[32] T. Chen, H. Liu, C. Deng, C. Zhou, P. Hong, Optimization and characterization of the gelatin/wheat gliadin nanofiber electrospinning process, Food Biophys. 17 (4) (2022) 621–634.
[33] X. Yang, D. Wu, Z. Du, R. Li, X. Chen, X. Li, Spectroscopy study on the interaction of quercetin with collagen, J. Agric. Food Chem. 57 (9) (2009) 3431–3435.
[34] H. Morris, R. Murray, Medical textiles, Text. Prog. 52 (1–2) (2020) 1–127.
[35] A.J. Capezza, Y. Cui, K. Numata, M. Lundman, W.R. Newson, R.T. Olsson, E. Johansson, M.S. Hedenqvist, Superabsorbent polymers: high capacity functionalized protein superabsorbents from an agricultural co-product: a cradle-to-cradle approach, Adv. Sustain. Syst. 4 (9) (2020) 2070018.
[36] A.J. Capezza, E. Robert, M. Lundman, W.R. Newson, E. Johansson, M. S. Hedenqvist, R.T. Olsson, Extrusion of porous protein-based polymers and their liquid absorption characteristics, Polymers 12 (2) (2020) 459.
[37] A.J. Capezza, M. Lundman, R.T. Olsson, W.R. Newson, M.S. Hedenqvist, E. Johansson, Carboxylated wheat gluten proteins: a green solution for production of sustainable superabsorbent materials, Biomacromolecules 21 (2020) 1709–1719.
[38] Y. Zhao, Y. Qiu, H. Wang, Y. Chen, S. Jin, S. Chen, Preparation of nanofibers with renewable polymers and their application in wound dressing, Int. J. Polym. Sci. 2016 (2016) 4672839.
[39] G. Liu, Z. Gu, Y. Hong, L. Cheng, C. Li, Electrospun starch nanofibers: recent advances, challenges, and strategies for potential pharmaceutical applications, J. Control. Release 252 (2017) 95–107.